JCTC Journal of Chemical Theory and Computation

Letter

pubs.acs.org/JCTC

Recovering Protein Thermal Stability Using All-Atom Hamiltonian Replica-Exchange Simulations in Explicit Solvent

Guillaume Stirnemann* and Fabio Sterpone*

CNRS Laboratoire de Biochimie Théorique, Institut de Biologie Physico-Chimique, Univ. Paris Denis Diderot, Sorbonne Paris Cité, PSL Research University, 13 rue Pierre et Marie Curie, 75005, Paris, France

Supporting Information

ABSTRACT: The REST2 method is successfully applied to investigate the thermal stability of chignolin CLN025 and of Trp-cage. As opposed to temperature replica exchange, REST2 relies on the rescaling of the protein potential energy, which allows a smaller number of replicas. The shape of the stability curve reconstructed on the basis of the corresponding-state principle is in very good agreement with experimental data; for chignolin, the effect of mutations is also recovered.

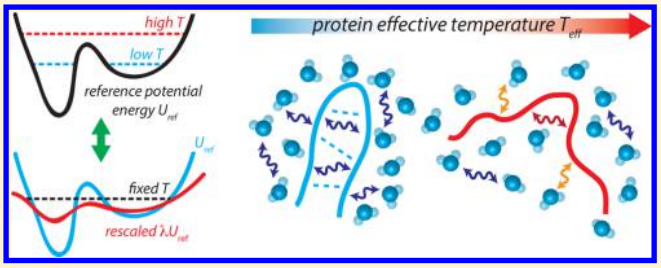

Adaptation to the environmental temperature has been a key driving mechanism of the proteome evolution.[1] Even today, some organisms known as extremophiles are found to thrive in environments much colder or much warmer than the human species comfort zone, spanning a temperature range of more than 120 °C. The molecular bases of such an adaptation are still being debated.[2] A main issue from a simulation perspective is that tackling protein thermostability with molecular dynamics (MD) remains challenging as the involved time scales for folding/unfolding events are usually long compared to the time scales readily accessible by simulations.[3,4] For example, stability differences between mesophilic/thermophilic homologues at very high yet still physical temperatures (e.g., 370 K) manifest only after hundreds of nanoseconds.[5] Moreover, when unfolding kinetics and mechanisms are of interest, the use of a stronger thermal stress, as routinely done, could lead to unphysical pathways.[6,7] A natural tool to accelerate sampling while assessing the protein response to temperature is to run parallel tempering — also referred to as temperature replica exchange — MD simulations (REMD).[8,9] A major drawback of this approach is that it is very sensitive to the overlap between the replicas total energies and thus to the system size. At the moment it is thus not applicable at an all-atom resolution in explicit solvent to proteins larger than a few tens of amino acids, as the number of required replicas rapidly becomes very large (tens of simulations). As an illustration, recent REMD simulations on the 20-residue Trp-cage, a small fast-folding protein, required 40 replicas propagated for hundreds of ns to obtain reasonable stability curves.[10]

As the energy overlap scales with the number of particles as $N^{-1/2}$, optimal exchange rate between replicas is limited by the number of solvent molecules that largely overpass the number of proteins sites. Because the main contributions to protein thermal unfolding are expected to be protein−protein and protein−solvent interactions, it is therefore tempting, among many other strategies,[9] to focus on these interactions only[11−14] in order to design alternative and computationally more effective sampling methods. These simulation schemes based on potential energy rescaling and Hamiltonian replica exchange are called solute-tempering, of which REST2[11] is a variant that we employ here. The corresponding state principle ensures an equivalent statistics between a system evolving at a reference potential energy and at a high temperature with a system evolving at a rescaled, smoothed potential energy and lower temperature. In REST2, since only the protein sites are affected, the scaling with total system size is much better as compared to standard REMD.[11] This approach has two main limitations, *a priori*. First, the thermodynamics is broken and can only be considered as exact at the chosen reference temperature; second, temperature-dependent solvent effects cannot be accounted for as the solvent always remains unperturbed at the reference temperature. Nonetheless, we present here an approach based on REST2 that is shown to be successful in determining protein stability curves in very good agreement with their experimental counterparts, just as REMD has been successful in that respect[10] while requiring a much larger number of replicas. We have implemented REST2 into NAMD 2.9[15] (we note that other implementations, especially in Gromacs,[16] exist), and we have been focusing on a mutant of the miniprotein chignolin, CLN025,[17] which exhibits a clear 2-state folding behavior and which has been studied by simulations[4] and experiments[17] in the past. When compared to the original design of chignolin,[18] which is much less stable at ambient temperature, CLN025 has a reasonably high melting temperature of 343 K.[17] We show that only a very moderate and reasonable number of replicas is required to yield to very good exchange rates and thus reasonable sampling, and we suggest a method to recover the protein stability curves. The success of our approach, which is applied to several

Received: June 29, 2015
Published: November 9, 2015

DOI: 10.1021/acs.jctc.5b00954
J. Chem. Theory Comput. 2015, 11, 5573−5577

miniproteins, is later demonstrated by comparing it to existing equilibrium MD and REMD results, together with the comparison with experimental thermodynamic data.

During a REST2 simulation, all replicas evolve at the same reference temperature β_{ref}, but the potential energy E_i of the ith replica is scaled as[11]

$$E_i(\vec{X}) = \lambda_i E_{pp}(\vec{X}) + \sqrt{\lambda_i} E_{pw}(\vec{X}) + E_{ww}(\vec{X}) \quad (1)$$

where $E_{pp}(\vec{X})$, $E_{pw}(\vec{X})$, and $E_{ww}(\vec{X})$ respectively designate the protein−protein, protein−water, and water−water potential energies. This nonlinear scaling of molecular interactions ensures an easy implementation with the usual mixing-rules and leads to a simple expression for the detailed balanced criterion. Following this definition, for each ith replica, REST2 defines 3 corresponding temperatures depending on the types of molecular interactions: protein−protein interactions evolve at $\beta_i = \lambda_i \beta_{ref}$; protein−water interactions evolve at $\beta_i = \sqrt{\lambda_i}\beta_{ref}$, and the solvent evolves at the reference temperature β_{ref}. As the main interest of REST2 is to sample protein folding, which mainly involves motions along the dihedral angle coordinates, only these bonded interactions along with nonbonded terms (usually Lennard-Jones and electrostatics) are rescaled[11] ($\lambda_i E_{pp}^{(1)}$). The protein bonds, angles, and impropers ($E_{pp}^{(2)}$) are left unperturbed so that the scaled total protein−protein interactions term in eq 1 is written as $E_{pp}^{\lambda_i} = \lambda_i E_{pp}^{(1)} + E_{pp}^{(2)}$. It follows from all these definitions that the scaled potential energy of $\lambda_i E_{pp}^{(1)}$ is achieved by rescaling the dihedral force constants and LJ energies of protein atoms by λ_i and their charges by $\sqrt{\lambda_i}$. The standard Lorentz−Berthelot mixing rules used for most force fields then lead to the expected scaling of $\sqrt{\lambda_i} E_{pw}(\vec{X})$ in eq 1.

Starting from previously equilibrated (folded) protein configurations of CLN025 in explicit solvent (see SI Text for details), we have performed REST2 simulations in the NVT ensemble at a reference physical temperature of β_{ref} = 300 K for 300 ns on 12 replicas exchanging the following protein−protein corresponding temperatures: 290, 300, 311, 322, 333, 345, 368, 394, 423, 455, 491, and 529 K. The CHARMM36[19] force field was employed for the protein solvated in TIP3P-CHARMM water molecules. Exchanges were attempted every 10 ps.

We first discuss the performance of exchange and sampling of the REST2 scheme for the CLN025 mutant (Figure 1A). Raw simulation data (replicas runing on separate physical processes exchange λ values) were first reordered according to a λ perspetive. In Figure 1B, we show the diffusion of some λ values in the replica space, suggesting that exploration of the full replica-space is achieved on a nanosecond time scale. Indeed, the exchange rate of success was found to be close to 57%. This high value is due to the very good overlap of the distributions of the energy factor relevant in the detailed balance factor, which can be approximated to $E_{pp}^{(1)}(\vec{X}) + (2\sqrt{\lambda_i})^{-1} E_{pw}(\vec{X})$,[11] whose distributions are shown in Figure 1C. For each λ, the distribution significantly overlaps with distributions in neighboring windows.

The trajectories in each λ window will sample the protein conformational free-energy surface with the corresponding, modified potential energy function (eq 1). The effect of the decreasing λ is analogous to an increase in the temperature and would therefore lead to a higher population of unfolded protein. This effect is illustrated in Figure 1D, where the

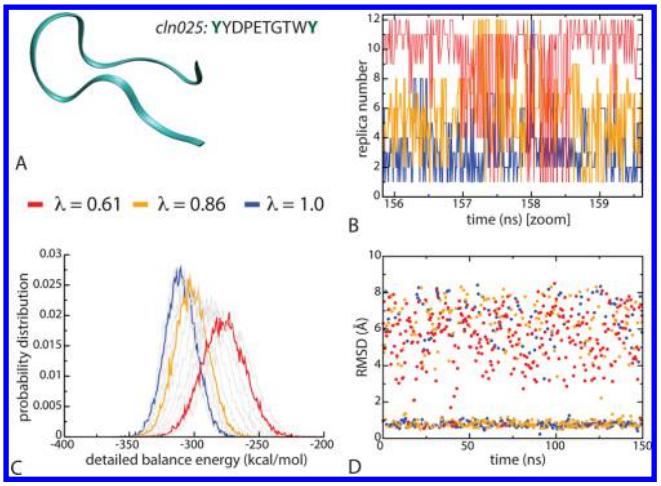

Figure 1. REST2 simulations of the CLN025 chignolin mutant, last 150 ns. (A) Schematic representation of chignolin CLN025, which folds as a small β-hairpin, and its amino-acid sequence. (B) Trajectories of some λ parameters (red: λ = 0.61; orange: λ = 0.86; blue: λ = 1.0) in the replica-space. Each λ visits all replicas within a few ns. (C) Distribution of the detailed balance energy relevant for exchange for the 12 values of λ. Some particular values are highlighted according to the color code of B. (D) Trajectories of the RMSD for the three values of λ. For clarity, two consecutive points are separated by 0.5 ns.

evolution of the backbone C_α root-mean-square displacement (RMSD) with respect to the center of the most populated cluster in the native state (see SI Text) is shown as a function of time for representative values of λ. For λ = 1, the protein evolves with its unperturbed potential energy at 300 K. Therefore, a significant population of folded conformation is found, as shown in Figure 1D where the corresponding RMSD takes values around 0.8 Å. At a smaller value of λ = 0.61 (protein−protein corresponding temperature of 491 K), the folded protein structure does not seem to be stable, and much higher values of the RMSD are observed (Figure 1D). Such time-profile of any reaction coordinate can be obtained for each λ and serves as a basis of subsequent free-energy surface reconstruction.

We now aim at using the REST2 simulation data to quantify the protein conformational response to temperature and to identify the key thermodynamical quantities of CLN025 folding equilibrium. The first step toward this goal is to adopt a consistent definition for the protein folded state, based on clustering techniques or cutoffs on given reaction coordinates. In Figure 2A, we compare two such variables. One is the standard RMSD defined above, whose cutoff is chosen to be 2 Å. As seen in Figure 1D, this value corresponds to a region of a conformational space which is very sparsely populated and very likely to be close to the folding reaction transition state region. It divides a compact region around 0.8 Å corresponding to the protein folded state and a very broad distribution around higher values corresponding to the protein unfolded conformations. As illustrated in Figure 2A, the observed thermal changes are almost identical if using a different reaction coordinate,[4] such as the smoothed fraction of native contacts Q (see SI text).

The thermodynamics in the reference window (λ = 1) is in principle exact and can be directly compared to experimental or simulation data at the same reference 300-K temperature. However, much more information would be obtained if one

DOI: 10.1021/acs.jctc.5b00954
J. Chem. Theory Comput. 2015, 11, 5573−5577

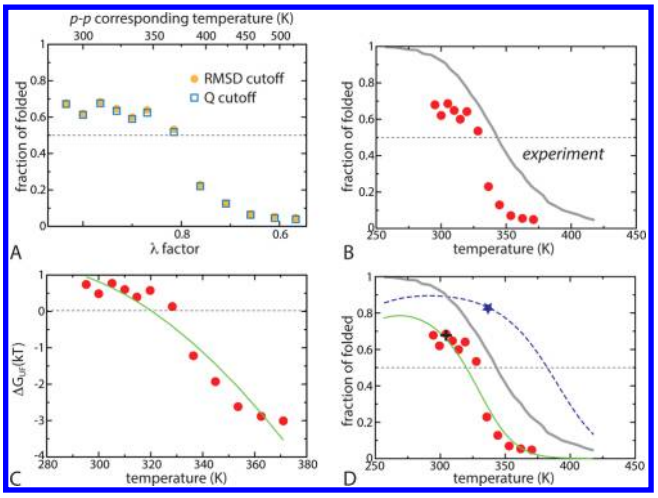

Figure 2. Stability curves of CLN025. (A) Fraction of folded conformations in each λ window. Cutoffs based on two different reaction coordinates (orange dots: C_α-RMSD; blue squares: number of contacts-based coordinate) give similar results. (B) Rescaling of the raw REST2 data (red circles) in terms of a corresponding temperature, as defined in the text, and comparison to the experimental curve (gray). (C) Unfolding free-energy calculated from the folded fraction curve (red circles) and analytical fit (green) leading to thermodynamical quantities. (D) Same plot but represented as the folded fraction as a function of temperature, compared to the experimental curve, the extrapolation of a 100-μs simulation published earlier (blue star—the extrapolation was made with the thermodynamical parameters suggested by the authors in the SI of ref 4) and the results of a simulated tempering study (black cross).[20]

could benefit from the other windows and convert the λ-scale into a physically relevant temperature range. We use the corresponding state principle to define the instantaneous, effective temperature β_i' in each frame of each window:

$$\beta_{ref} E_i(\vec{X}) = \beta_i' E_{ref}(\vec{X}) \tag{2}$$

Since we are mainly interested in the effective corresponding temperature for the protein conformational equilibrium, we neglect the unscaled bath E_{ww} contribution. The effective temperature therefore results from a balance between the scaled energies E_{pp} and E_{pw}:

$$\langle \beta_i' \rangle = \beta_i \left(1 + \left(\sqrt{\frac{\beta_{ref}}{\beta_i}} - 1 \right) \left\langle \frac{E_{pw}(\vec{X})}{E_{pp}(\vec{X}) + E_{pw}(\vec{X})} \right\rangle \right) \tag{3}$$

A derivation of this equation based on a mean-field approach and the corresponding approximations are given in the SI. The resulting formulation clearly highlights the asymptotic behavior of $\langle \beta_i' \rangle$, which is equal to β_i if $E_{pw} \ll E_{pp}$ and to $\sqrt{\beta_i \beta_{ref}}$ if $E_{pw} \gg E_{pp}$, which follows eq 1. For the small protein chignolin, the protein−protein interactions are small compared to their protein−solvent counterpart. A direct consequence is that the simulation corresponding temperature range [280−529] K for protein−protein interactions translates into an effective temperature range of ≈[290−370] K, as seen in Figure 2B. As we now have a physically relevant temperature range, comparison with experimental data[17] can be made (Figure 2B, gray curve). While the REST2 simulations slightly underestimate the protein stability as a function of temperature (shift of ≈20 K), the overall shape and temperature dependence are very well reproduced by our approach. This can be compared with the results of much more expensive, standard REMD simulations[21] or extrapolations made from very long equilibrium trajectories at one temperature only,[4] as discussed later.

To allow more quantitative comparison with experiments, we have extracted thermodynamic data from our simulations using the general Hawley's expression[22] for the free-energy difference between the folded and the unfolded state, derived from the fraction of folded protein using Boltzmann statistics, and which can be written as[22,23]

$$\Delta G(T) = -\Delta C_v \left[T\left(\ln\left(\frac{T}{T_m} \right) - 1 \right) + T_m \right] + \Delta H_m \left(1 - \frac{T}{T_m} \right) \tag{4}$$

where T_m is the melting temperature, ΔC_v is the change in heat capacity when going from folded to unfolded (considered as constant), and ΔH_m is the melting enthalpy. Fitting the free-energies of protein unfolding (Figure 2C, green) leads to an estimate of these thermodynamic quantities that can be directly compared with the experimental values (Table I). The melting temperature is well-predicted but slightly underestimated by ≈20 K (without the fit, the point at $T \approx 328$ K actually exhibits a fraction of folded protein close to 50%). The melting enthalpy as well as the unfolding free-energy differs from the experimental values by 1 kcal/mol, and despite being of a different sign, ΔC_v remains very small, as expected (the fit of the experimental data in ref 17 is actually performed assuming $\Delta C_v = 0$). We note a clear difference between our results and the extrapolation based on a very long (100 μs) brute force MD simulation at 340-K published by the DE Shaw group.[4] The value of the unfolding free-energy at the experimental melting temperature $T_m^{exp} = 343$ K (Table I) illustrates this difference. At this temperature REST2 simulations estimate a lower fraction of folded protein as compared to the experiments, while according to the extrapolation of the μs-simulation,[4] the protein is overstabilized (Figure 2D). Besides differences in the methodologies and their sampling efficiencies, we also note that the employed force fields are slightly different, although they are both based on recently reparametrized versions of CHARMM (CHARMM36 vs CHARMM22*[4]). Interestingly, a very recent simulated-tempering (ST) study using CHARMM22*[20] found that the fraction of folded state at 310 K was ≈67%, which is in very good agreement with our stability curve but much below the extrapolation of ref 4 (black cross in Figure 2D).

Table I. Thermodynamic Parameters Extracted from Different Sets of Available Data[a]

system	T_m (K)	ΔH_m (kcal/mol)	ΔC_v (kcal/mol/K)	$\Delta G(300)$ (kcal/mol)	$\Delta G(T_m^{exp})$ (kcal/mol)
expt	343	+10.5	−0.07	+1.5	0
REST2	321	+9.4	+0.17	+0.5	−0.8
MD(μs)	382	+9.7	+0.10	+1.1	+0.8

[a]Experiments: fit of the stability curve using eq 4, ref 17, and Figure 2B; current work: fit of the stability curve (Figure 2C); MD(μs): extrapolation of a 100-μs simulation at 340 K using eq 4 and data in the SI of ref 4.

We have also repeated REST2 simulations on the first design of chignolin[18] here referred to as CLN001, which only differs by the two terminal residues that are both replaced by glycine. Experimentally, this peptide is only marginally stable at ambient temperature, with a melting temperature around 310 K.[18] At

DOI: 10.1021/acs.jctc.5b00954
J. Chem. Theory Comput. 2015, 11, 5573−5577

ambient condition the mutant CLN025 is about 1 kcal/mol more stable than CLN001. As detailed in the SI, our simulations reproduce this trend as there is a dramatic shift of stability toward lower temperatures. This stability shift is also recovered by computing the free energy associated with the mutations G1Y/G10Y via alchemical free-energy (shown in the SI). However, in practice these "single-point" calculations cannot fully sample the folded/unfolded state conformational ensemble; thus they do not provide the associated mechanistic details, and they are performed at a given thermodynamic condition. Therefore, REST2 appears as a valuable tool to contrast the behavior and to recover temperature dependent quantities of several mutants that exhibit distinct thermal stabilities.

We finally discuss the convergence of the results, and we compare it to a more standard simulation scheme based on temperature exchange among replicas. In Figure 3A, we show

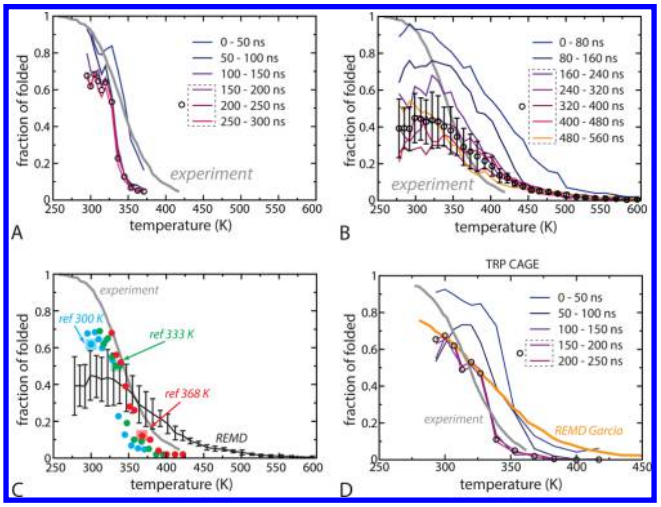

Figure 3. Comparison between REST2, REMD, and experiments. Stability curves of CLN025 using REST2 (A) taken in successive blocks of 50 ns along a 300 ns trajectory (colored lines) and comparison to experimental data (gray). The average over the last 150 ns is shown as black circles (data reported in Figure 2). Standard deviation is very small and is not indicated. Comparison with REMD data (B) using 32 replicas between 278 and 600 K, propagated for 560 ns, and shown for blocks of 80 ns. The average over the last 400 ns portion of the trajectories is shown as black circles, and the standard deviation among the 5 corresponding blocks is shown. (C) Comparison between the average stability curves obtained in REMD (black line with error bars) and in REST2 at a reference temperature of 300 K (blue circles), 333 K (green circles), and 368 K (red circles). (D) Stability curves of Trp-cage obtained using REST2 (black circles — averaged over the last 100 ns of the simulation), REMD from the Garcia group[10] (orange) and in the experiments (gray).[10]

the evolution of the fraction of folded configurations along the 300 ns trajectory, based on 50 ns block-averages. The stability curve is observed to be stable after ≈150 ns, and we have used the subsequent portion of the trajectory for the data presented above. Although we cannot make sure that the stability curve will no further evolve on a much larger time scale, these results can be compared to those of the standard REMD scheme. Despite a much larger number of replicas (32 vs 12 for REST2), which is required to ensure a decent exchange rate (close to 30% in that case), convergence is much slower, and, quite strikingly, the melting curve exhibits large fluctuations even after more than 500 ns (Figure 3B). Previous simulations on CLN001 have reported convergence of the data on the 300−500 ns time scale,[24] and REMD simulations of the miniprotein Trp-cage were also observed to converge on a similar time scale.[10]

By averaging on the portion of the REMD simulation where the fraction of folded state among replicas seems to fluctuate around an average value (we chose 160−560 ns), we can further compare the stability curves obtained by REST2, REMD, and in the experiments (Figure 3C). The overall shape of the REMD stability curve is more spread than the experimental one, and a marginal stability of the protein at unphysically high temperatures (400 K and above) is observed. This behavior was reported for chignolin CLN001 with 4 different force fields[21] and for Trp-cage.[10] This significant disagreement may be due to the temperature-dependence of the protein and the water force fields that were mostly parametrized to reproduce ambient-temperature properties. Together with the effective way of recovering the temperature scale in the REST2 approach (where the simulation temperature is similar among replicas), this may explain the differences between the REST2 and REMD stability curves at high temperatures. However, at the reference simulation temperature, the thermodynamics is exact, and all simulation strategies should lead to the same results, assuming they are converged. When this reference temperature is 300 K, the fraction of folded states observed in the unperturbed window of the REST2 simulations is actually close to the edge of the error bars (10%) of the REMD simulation (blue square in Figure 3C). (We note that in REMD simulations of Trp-cage, fluctuations of about 10% of the total fraction (summed over all replicas) of folded configurations were still observed beyond 600 ns of simulation per replica[10]). As already noted, our results are in very good agreement with a previous ST study using a very similar force field,[20] and it is worth stressing here that ST has been shown to be more efficient than REMD in terms of convergence.[25]

In order to control the effect of bath thermalization, we have also carried out REST2 simulations using higher reference temperatures for the solvent (333 and 368 K, see the SI for details). As shown in Figure 3C, the fraction of folded states in the corresponding unperturbed windows is close to the (large) fluctuations observed in the REMD simulations. Another interesting feature of the corresponding stability curves, which will be examined in more detail in a future work, is that although slightly shifted, they are not dramatically different from that at 300 K, further validating our effective temperature reconstruction and suggesting that, at least for this system, temperature-dependent solvent effects only bring minor contributions in the physical temperature range $T < 400$ K (the shift in the estimated melting temperature is <20 K, while the reference temperature changes by 68 K).

To further reinforce this comparison between REMD, REST2, and experiments, we have performed simulations of another miniprotein, Trp-cage, for which converged REMD simulations extending at the microsecond time scale per replica have been reported in the literature.[10] For this system, the CHARMM36 force field lead to very poor agreement with experiments, and we had to use the Amberff99SB[26] protein force field (see the SI for details). As shown in Figure 3D, the REST2 simulations seem to be converged on a 250 ns time scale, and the resulting stability curve agrees very well with that obtained with REMD at temperatures close to 300 K, where solvent-specific temperature effects and approximations due to

DOI: 10.1021/acs.jctc.5b00954
J. Chem. Theory Comput. 2015, 11, 5573−5577

the temperature reconstruction in REST2 are more modest as compared to the highest temperatures for which REST2 markedly differs from REMD. However, the agreement between REST2 and experimental data is excellent.

In conclusion, we have implemented a solute-scaling Hamiltonian-exchange algorithm, REST2, that was successfully applied to the study of miniprotein thermal stability. A strategy was suggested in order to recover an effective temperature-scale. Only a very limited number of replicas (12), simulated for up to 300 ns each, was necessary to obtain a stability curve in very good agreement with experimental data. In particular, the simulated melting temperature for chignolin CLN005 is close to the experimental one, differing by only ≈20 K. The experimental shift in chignolin stability upon mutation was also reproduced by our simulations, and our approach was also successful in reproducing the thermal stability of the 20-residue Trp-cage. We are currently deploying this methodology to investigate larger protein systems to uncover some of the thermodynamical and molecular features of protein thermo-stability.

■ ASSOCIATED CONTENT

Supporting Information

The Supporting Information is available free of charge on the ACS Publications website at DOI: 10.1021/acs.jctc.5b00954.

Details about the simulations, the definition of collective variables, the alchemical free-energy calculations, and justification of eq 3 (PDF)

■ AUTHOR INFORMATION

Corresponding Authors

*E-mail: stirnemann@ibpc.fr.

*E-mail: sterpone@ibpc.fr.

Notes

The authors declare no competing financial interest.

■ ACKNOWLEDGMENTS

The research leading to these results has received funding from the European Research Council under the European Community's Seventh Framework Programme (FP7/2007-2013) Grant Agreement no. 258748. Part of his work was performed using HPC resources from GENCI [CINES and TGCC] (Grant x201476818/x201576818). We acknowledge the financial support for infrastructures from ANR-11-LABX-0011-01.

■ REFERENCES

(1) Boussau, B.; Blanquart, S.; Necsulea, A.; Lartillot, N.; Gouy, M. Parallel adaptations to high temperatures in the Archaean eon. *Nature* **2008**, *456*, 942−945.

(2) Sterpone, F.; Melchionna, S. Thermophilic proteins: insight and perspective from in silico experiments. *Chem. Soc. Rev.* **2012**, *41*, 1665−1676.

(3) Dill, K. A.; MacCallum, J. L. The protein-folding problem, 50 years on. *Science* **2012**, *338*, 1042−1046.

(4) Lindorff-Larsen, K.; Piana, S.; Dror, R. O.; Shaw, D. E. How fast-folding proteins fold. *Science* **2011**, *334*, 517−520.

(5) Kalimeri, M.; Rahaman, O.; Melchionna, S.; Sterpone, F. How conformational flexibility stabilizes the hyperthermophilic elongation factor G-domain. *J. Phys. Chem. B* **2013**, *117*, 13775−13785.

(6) Huang, X.; Zhou, H.-X. Similarity and difference in the unfolding of thermophilic and mesophilic cold shock proteins studied by molecular dynamics simulations. *Biophys. J.* **2006**, *91*, 2451−2463.

(7) Wang, T.; Wade, R. C. On the use of elevated temperature in simulations to study protein unfolding mechanisms. *J. Chem. Theory Comput.* **2007**, *3*, 1476−1483.

(8) Sugita, Y.; Okamoto, Y. Replica-exchange molecular dynamics method for protein folding. *Chem. Phys. Lett.* **1999**, *314*, 141−151.

(9) Abrams, C.; Bussi, G. Enhanced sampling in molecular dynamics using metadynamics, replica-exchange, and temperature-acceleration. *Entropy* **2014**, *16*, 163−199.

(10) Day, R.; Paschek, D.; Garcia, A. E. Microsecond simulations of the folding/ unfolding thermodynamics of the Trp-cage miniprotein. *Proteins: Struct., Funct., Genet.* **2010**, *78*, 1889−1899.

(11) Wang, L.; Friesner, R. A.; Berne, B. J. Replica exchange with solute scaling: A more effcient version of replica exchange with solute tempering (REST2). *J. Phys. Chem. B* **2011**, *115*, 9431−9438.

(12) Liu, P.; Kim, B.; Friesner, R. A.; Berne, B. J. Replica exchange with solute tempering: a method for sampling biological systems in explicit water. *Proc. Natl. Acad. Sci. U. S. A.* **2005**, *102*, 13749−13754.

(13) Moors, S. L. C.; Michielssens, S.; Ceulemans, A. Improved replica exchange method for native-state protein sampling. *J. Chem. Theory Comput.* **2011**, *7*, 231−237.

(14) Terakawa, T.; Kameda, T.; Takada, S. On easy implementation of a variant of the replica exchange with solute tempering in GROMACS. *J. Comput. Chem.* **2011**, *32*, 1228−1234.

(15) Phillips, J. C.; Braun, R.; Wang, W.; Gumbart, J.; Tajkhorshid, E.; Villa, E.; Chipot, C.; Skeel, R. D.; Kalé, L.; Schulten, K. Scalable molecular dynamics with NAMD. *J. Comput. Chem.* **2005**, *26*, 1781−1802.

(16) Bussi, G. Hamiltonian replica exchange in GROMACS: a flexible implementation. *Mol. Phys.* **2014**, *112*, 379−384.

(17) Honda, S.; Akiba, T.; Kato, Y. S.; Sawada, Y.; Sekijima, M.; Ishimura, M.; Ooishi, A.; Watanabe, H.; Odahara, T.; Harata, K. Crystal structure of a ten-amino acid protein. *J. Am. Chem. Soc.* **2008**, *130*, 15327−15331.

(18) Honda, S.; Yamasaki, K.; Sawada, Y.; Morii, H. 10 Residue folded peptide designed by segment statistics. *Structure* **2004**, *12*, 1507−1518.

(19) Huang, J.; MacKerell, A. D. CHARMM36 all-atom additive protein force field: Validation based on comparison to NMR data. *J. Comput. Chem.* **2013**, *34*, 2135−2145.

(20) Zhang, T.; Nguyen, P. H.; Nasica-Labouze, J.; Mu, Y.; Derreumaux, P. Folding atomistic proteins in explicit solvent using simulated tempering. *J. Phys. Chem. B* **2015**, *119*, 6941−6951.

(21) Kührová, P.; De Simone, A.; Otyepka, M.; Best, R. B. Force-field dependence of chignolin folding and misfolding: Comparison with experiment and redesign. *Biophys. J.* **2012**, *102*, 1897−1906.

(22) Hawley, S. A. Reversible pressure-temperature denaturation of chymotrypsinogen. *Biochemistry* **1971**, *10*, 2436−2442.

(23) Becktel, W. J.; Schellman, J. A. Protein stability curves. *Biopolymers* **1987**, *26*, 1859−1877.

(24) Seibert, M. M.; Patriksson, A.; Hess, B.; Van Der Spoel, D. Reproducible polypeptide folding and structure prediction using molecular dynamics simulations. *J. Mol. Biol.* **2005**, *354*, 173−183.

(25) Nguyen, P. H.; Okamoto, Y.; Derreumaux, P.; Ngyuen, P. H. Communication: Simulated tempering with fast on-the-fly weight determination. *J. Chem. Phys.* **2013**, *138*, 061102.

(26) Hornak, V.; Abel, R.; Okur, A.; Strockbine, B.; Roitberg, A.; Simmerling, C. Comparison of multiple Amber force fields and development of improved protein backbone parameters. *Proteins: Struct., Funct., Genet.* **2006**, *65*, 712−725.

DOI: 10.1021/acs.jctc.5b00954
J. Chem. Theory Comput. 2015, 11, 5573−5577